Electronic Supplementary Material (ESI) for Journal of Materials Chemistry C.

Electronic Supplementary Information for

Benzothiazolium-functionalized NU-1000: a versatile material for carbon dioxide adsorption and cyanide luminescence sensing

Lapo Luconi,[a] Giorgio Mercuri,[a] Timur Islamoglu,[b] Andrea Fermi,[c,] Giacomo Bergamini,[c] Giuliano Giambastiani,[a,d,e,]* and Andrea Rossin [a,]**

[a] *Istituto di Chimica dei Composti Organometallici (ICCOM-CNR),Via Madonna del Piano 10, 50019 Sesto Fiorentino, Italy.*

[b] *Department of Chemistry, Northwestern University 2145 Sheridan Road, Evanston, IL 60208, United States.*

[c] *Dipartimento di Chimica "G. Ciamician", Università di Bologna, via Selmi 2, 40126 Bologna, Italy.*

[d] *Institute of Chemistry and Processes for Energy, Environment and Health (ICPEES), UMR 7515 CNRS-University of Strasbourg (UdS), 25, rue Becquerel, 67087 Strasbourg Cedex 02, France.*

[e] *Kazan Federal University, Alexander Butlerov Institute of Chemistry, 420008 Kazan, Russian Federation.*

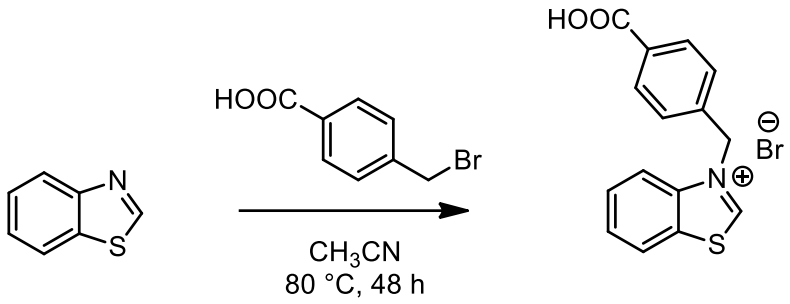

Scheme S1. Synthesis of **BzTz**.

Single-crystal X-ray Diffraction Structure Determination of BzTz

Single crystal X-Ray data were collected at low temperature (T = 100 K) on a Bruker APEX-II CCD diffractometer using a Cu Kα radiation (λ = 1.5418 Å). The program used for the data collection and reduction was the Bruker SAINT software package. Data were corrected for absorption effects using the Multi-Scan method (SADABS). Direct methods implemented in Sir2014[1] were used to solve the structures and the refinements were performed by full-matrix least-squares against F^2 implemented in SHELXL-2018.[2] All the non-hydrogen atoms were refined anisotropically while the hydrogen atoms were fixed in calculated positions and refined isotropically with the thermal factor depending on the one of the atom to which they are bound. The –COOH hydrogen atom was located on the residual density maps and then included with fixed bond distances and U_{iso} values constrained at the level of $1.5 \times U_{eq}$ of the carrier oxygen atom. The geometrical calculations were performed by PARST97[3] and molecular plots were produced by the program ORTEP3.[4] CCDC-1988747 contains the supplementary crystallographic data for **BzTz**. These data can be obtained free of charge from The Cambridge Crystallographic Data Centre *via* https://www.ccdc.cam.ac.uk/structures/. Table S1 collects the main experimental details and crystallographic data.

Table S1. Main crystallographic data, experimental details and structure refinement details for **BzTz**.

Formula	C_{15} H_{12} Br N O_2 S
M [g mol^{-1}]	350.23
T [K]	100
Color, habit	Colorless prisms
Size [mm^3]	0.01 x 0.01 x 0.02
Crystal system	Monoclinic
a [Å]	7.3944(5)
b [Å]	14.8659(9)
c [Å]	13.0018(8)
β [°]	91.5700(10)
V [$Å^3$]	1428.68(16)
D_{calc} [g cm^{-3}]	1.628
Space group	$P2_1/c$
Z	4
θ range for collection [°]	28.493 to 74.563
Measured reflns	2174
Unique reflns	1666
Completeness [%]	58.5 %
R_{int}	0.0273
Data/restraints/parameters	1666 / 0 / 184
*R*1, w*R*2 [$I > 2\sigma(I)$]	0.0528, 0.1534
*R*1, w*R*2 (all data)	0.0530, 0.1537
Gof on F^2	1.213
Max, min peak [e $Å^{-3}$]	0.758, -0.952

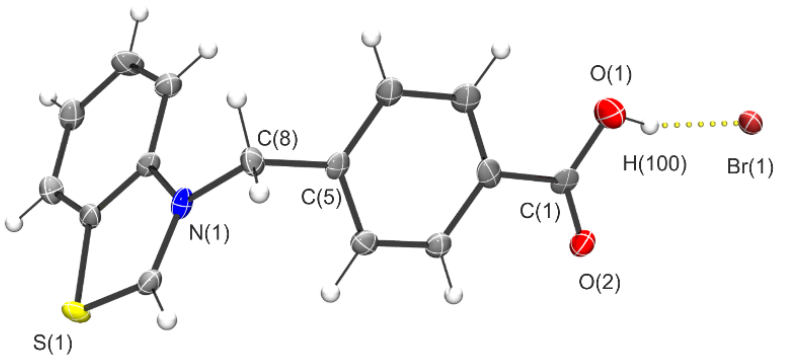

Figure S1. ORTEP drawing of **BzTz** at 70% probability level. Selected bond lengths (Å) and angles (°): C(8)-N(1) = 1.481(6); C(1)-O(1) = 1.328(6); C(1)-O(2) = 1.222(7); O(1)-H(100) = 0.96(13); N(1)-C(8)-C(5) = 110.3(5). Hydrogen bonds [D---A distances (Å)]: O(1)-H(100)...Br(1) = 3.190(4).

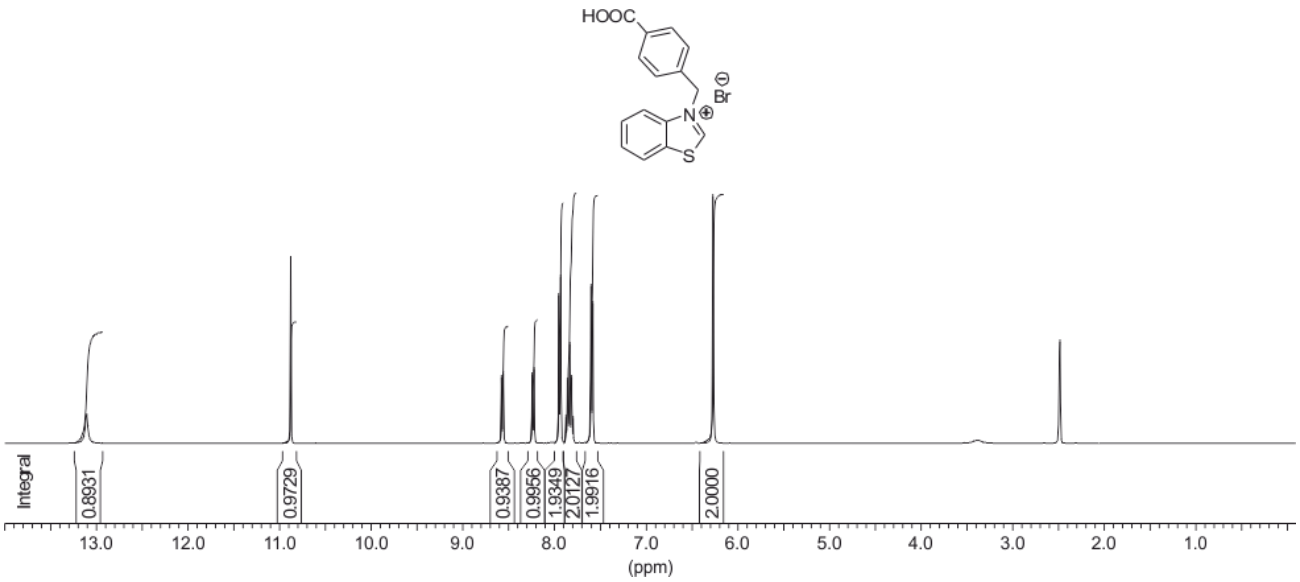

Figure S2. ^{1}H NMR spectrum (400 MHz, DMSO-d_6, 298K) of **BzTz**.

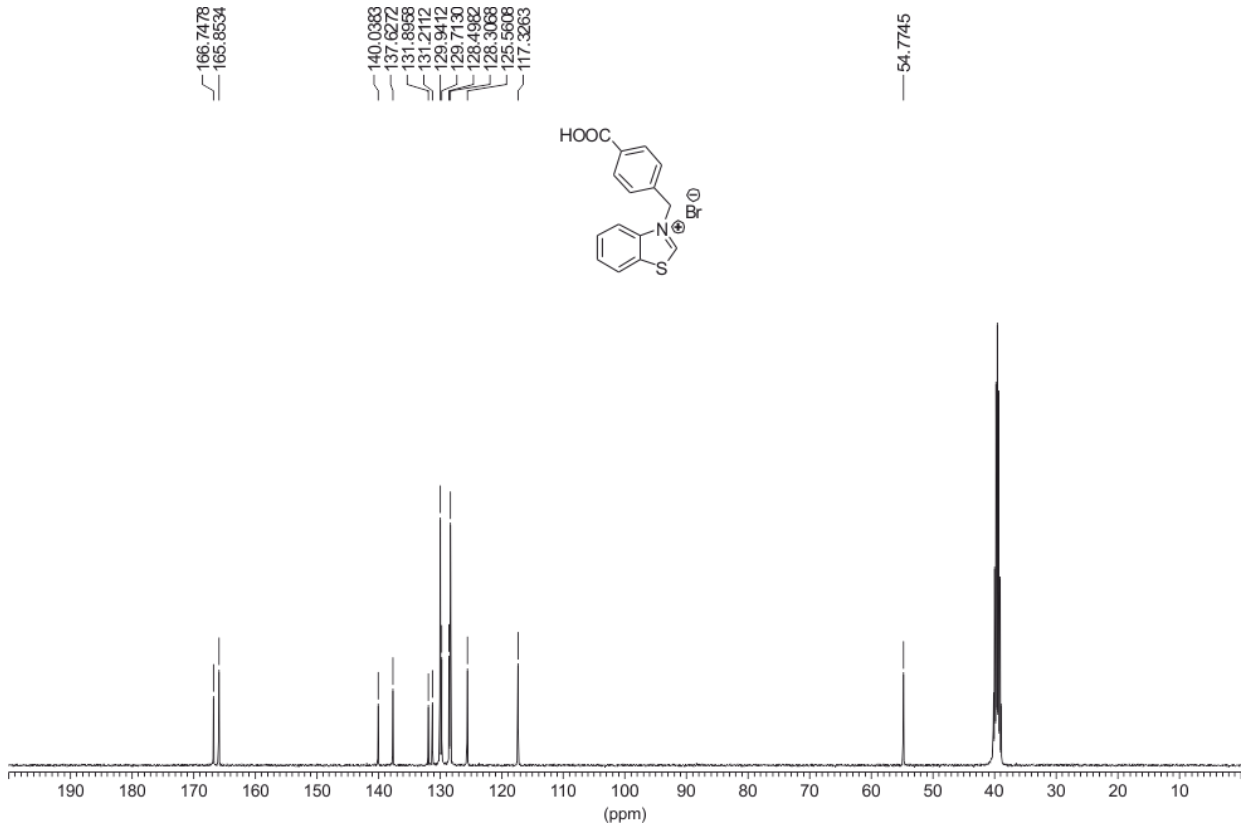

Figure S3. ^{13}C{^{1}H} NMR spectrum (100 MHz, DMSO-d_6, 298K) of **BzTz**.

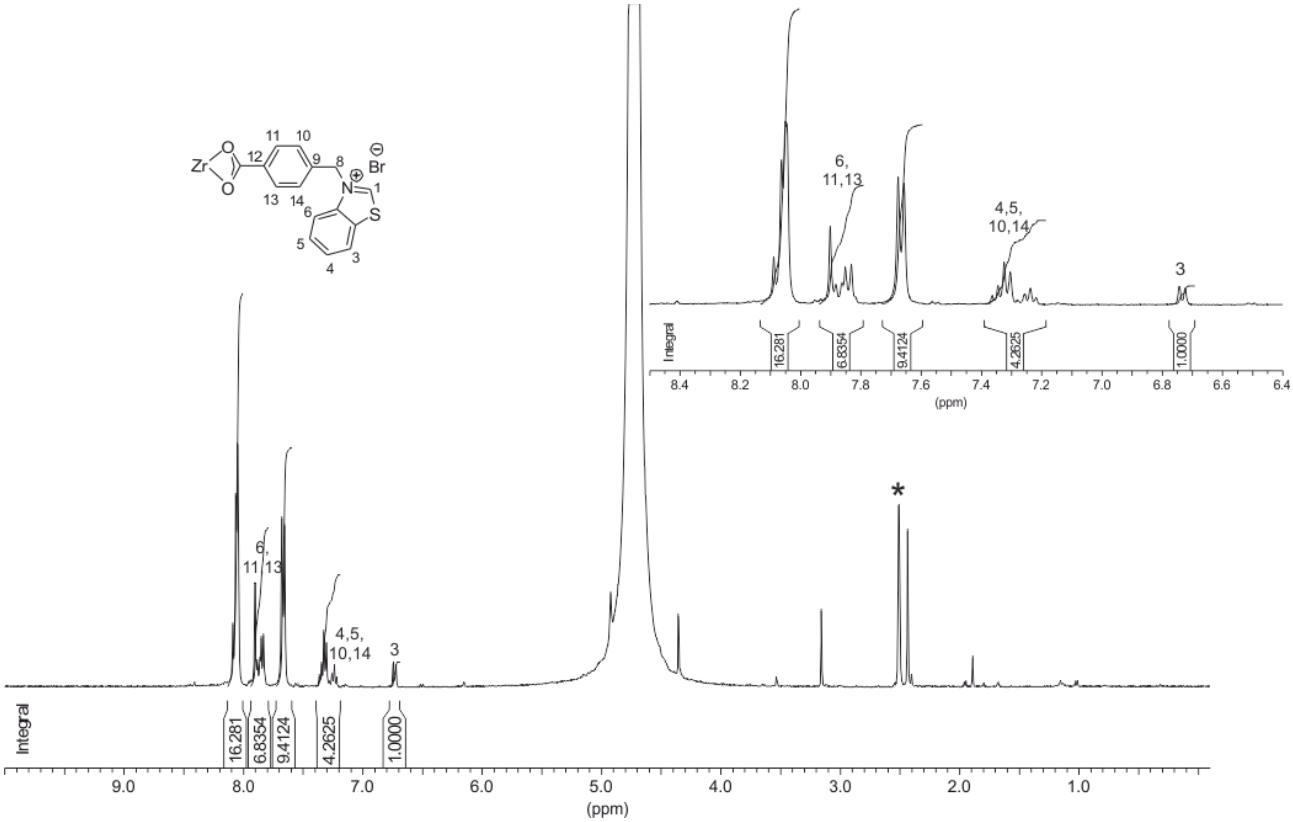

Figure S4. ^{1}H NMR spectrum (400 MHz, 5 % HF-DMSO-d_6, 298K) of the digested **NU-1000-BzTz**. *residual DMSO solvent peak. Inset: zoom of the aromatic region used for the quantification of the functionalization degree.

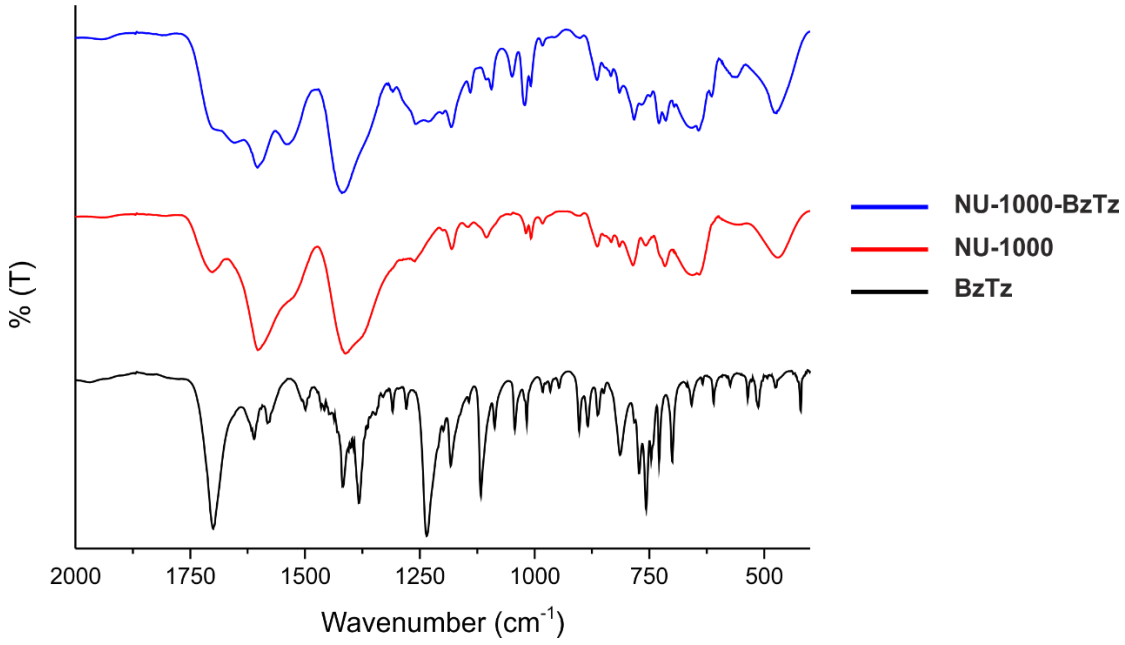

Figure S5. Infrared spectra (KBr, T = 298 K) of **BzTz**, **NU-1000** and their combination at comparison.

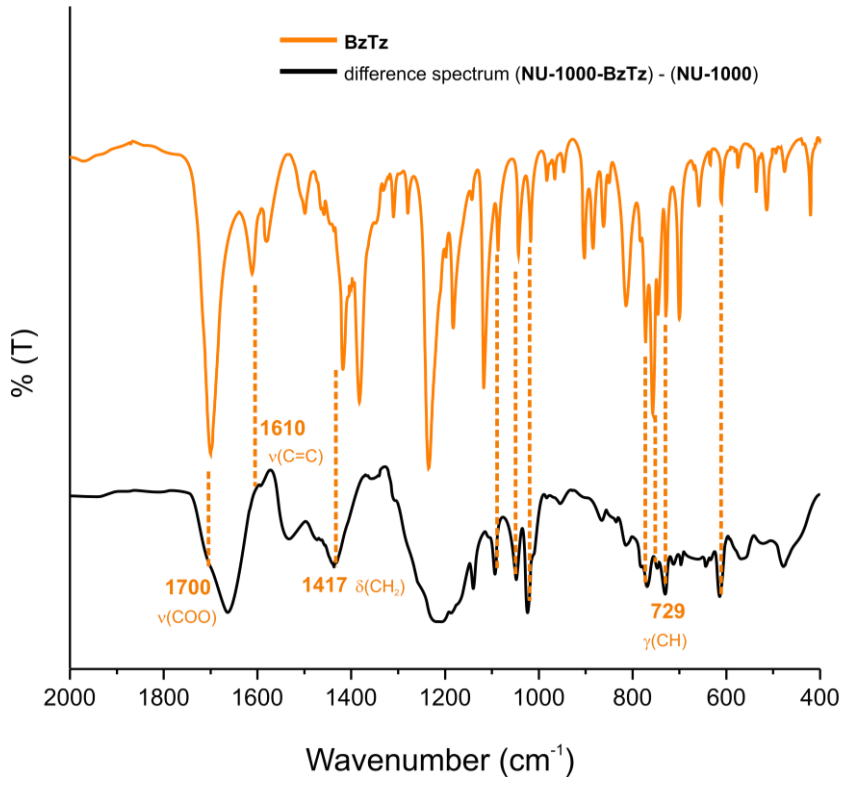

Figure S6. Infrared [(**NU-1000-BzTz)-(NU-1000)**] difference spectrum (KBr, T = 298 K, black) and **BzTz** spectrum (KBr, T = 298 K, orange) at comparison. Some typical benzothiazolium normal modes are highlighted thgrough orange dotted lines.

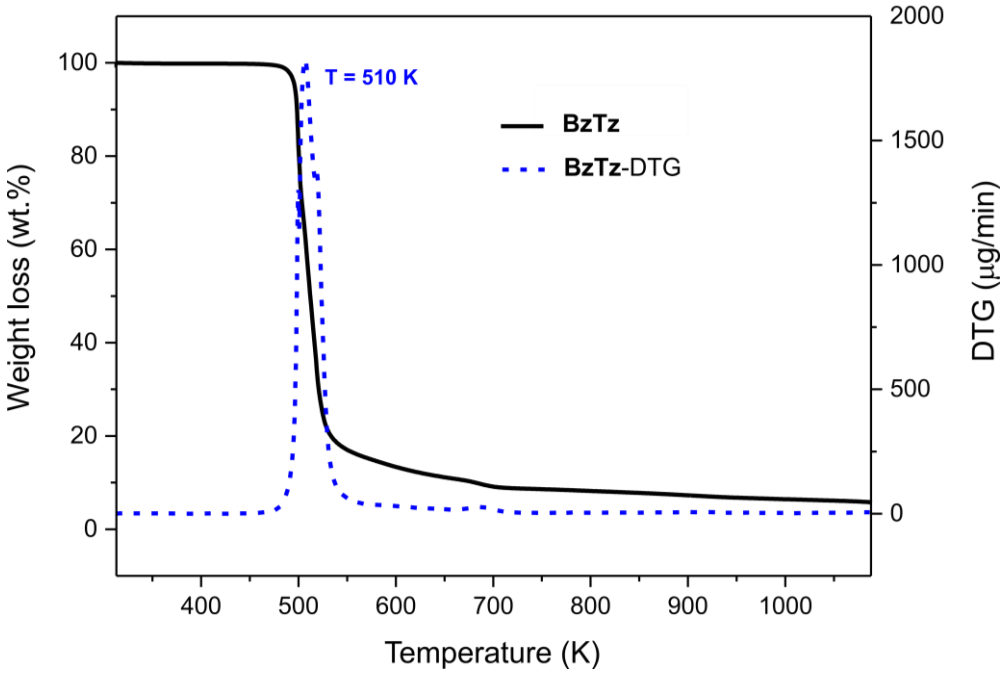

Figure S7. Thermogravimetric analysis *vs.* time profile of **BzTz**.

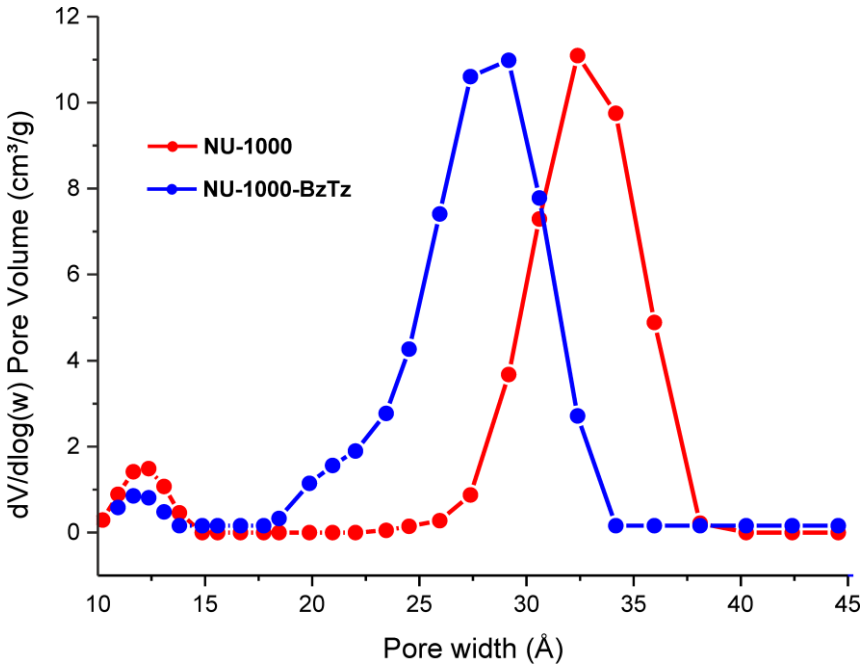

Figure S8. NLDFT (Tarazona model for cylindrical pores) pore size distribution of **NU-1000** and **NU-1000-BzTz** at comparison.

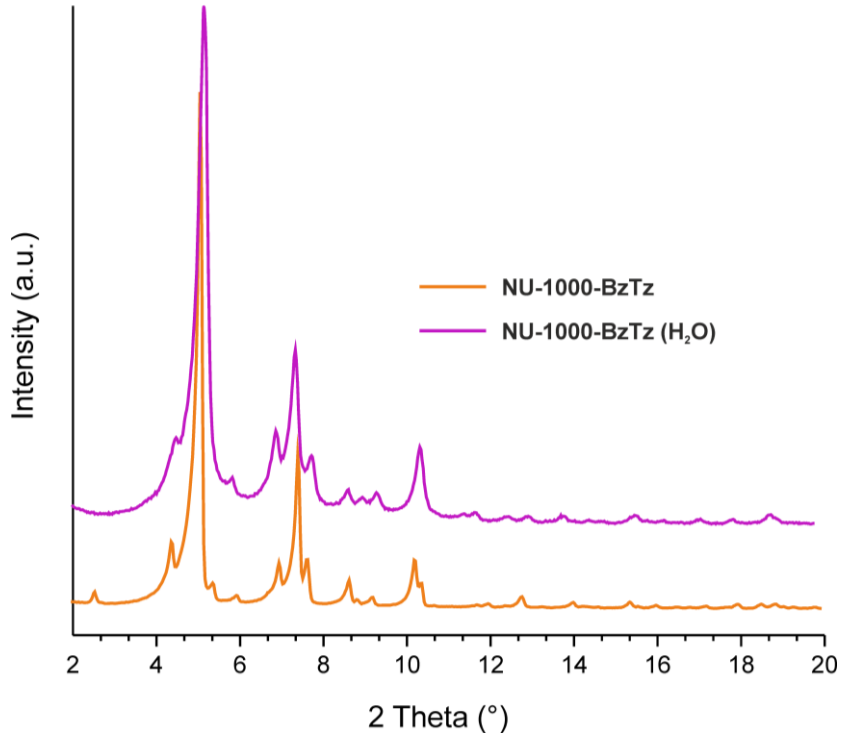

Figure S9. PXRD profiles of the as-synthesized **NU-1000-BzTz** (orange) and after soaking in water for 24 hours at ambient temperature (purple).

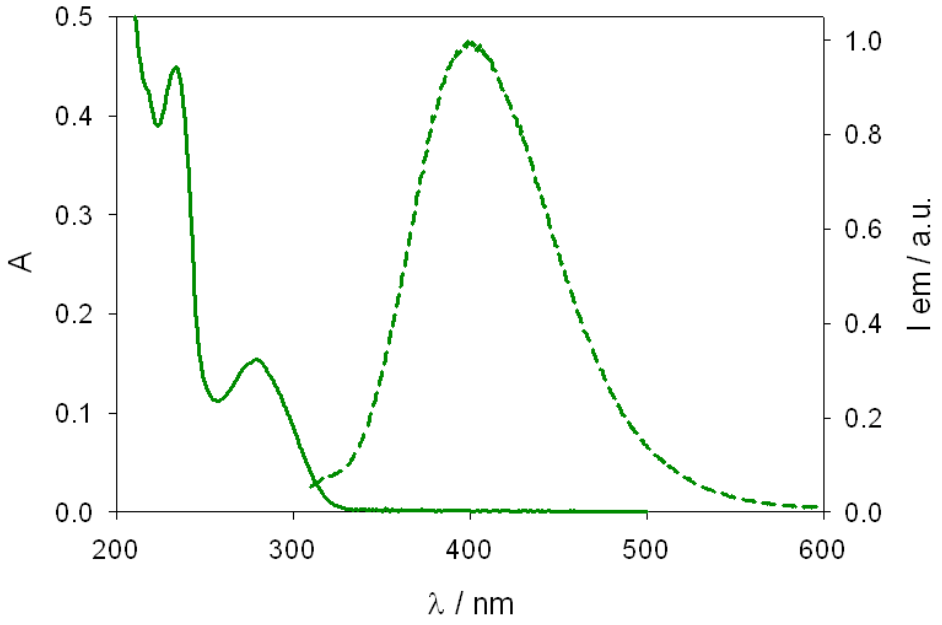

Figure S10. Qualitative absorption (solid line) and normalized emission spectra (dashed line) of **BzTz** in H_2O at r.t. λ_{ex}=280 nm.

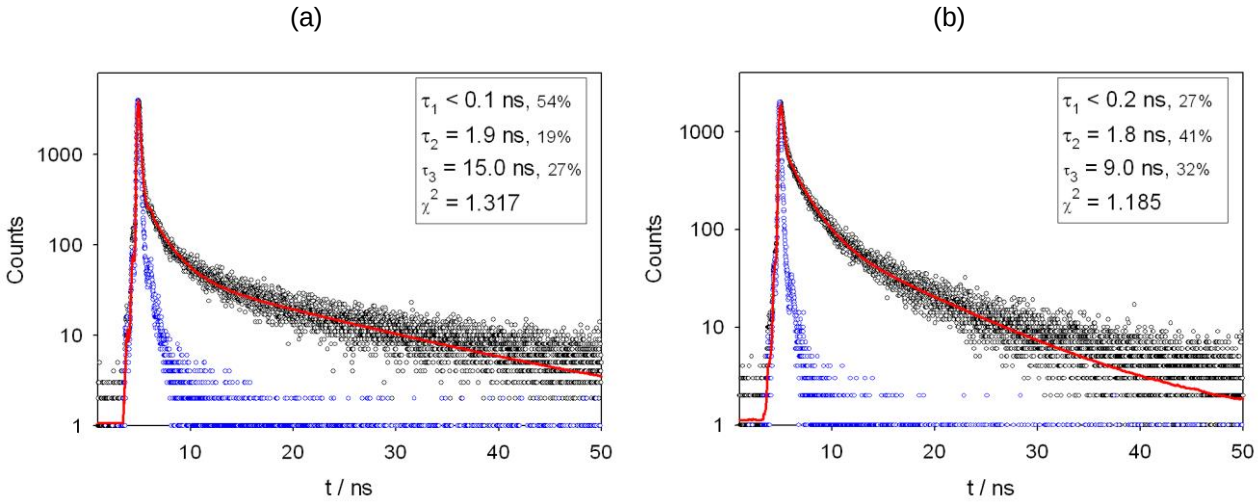

Figure S11. (a) Fluorescence decay of **NU-1000** in aqueous suspensions at r.t. The decay is fitted with a triexponential function (red line); the instrument response function is also shown (black dots). λ_{ex}=405 nm, λ_{em}=450 nm. (b) Fluorescence decay of **NU-1000-BzTz** in aqueous suspensions at r.t. The decay is fitted with a triexponential function (red line); the instrument response function is also shown (black dots). λ_{ex}=405 nm, λ_{em}=520 nm.

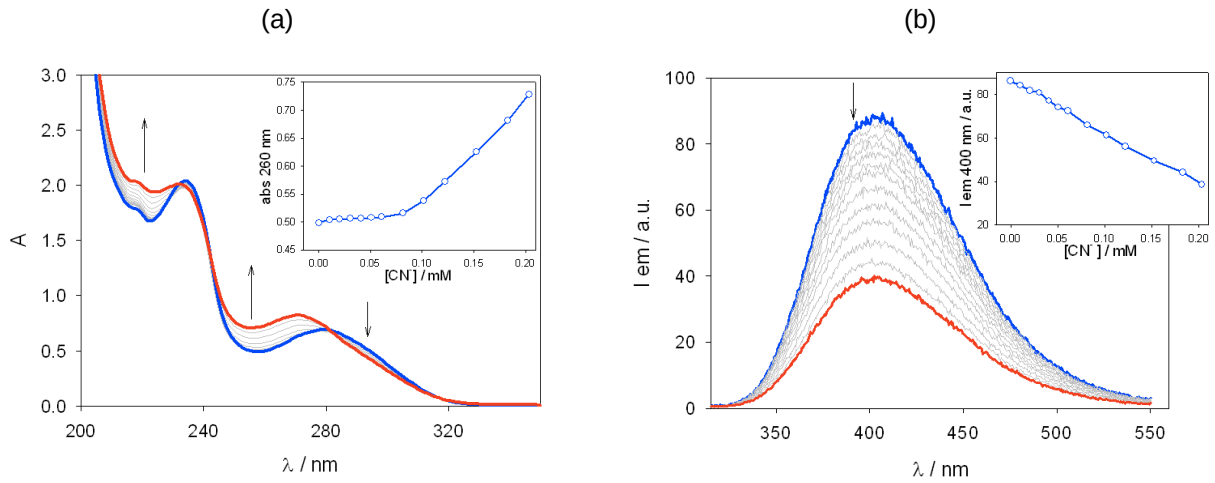

Figure S12. (a) Evolution of the absorption spectra recorded for a solution of **BzTz** ($1.05 \cdot 10^{-4}$ M) in water upon additions of KCN. Inset: absorption profile at 260 nm. (b) Evolution of the emission spectra recorded for a solution of **BzTz** ($1.05 \cdot 10^{-4}$ M) in water upon additions of KCN. Inset: emission intensity profile at 400 nm. The emission spectra are not corrected for absorption changes at λ_{ex}=275 nm.

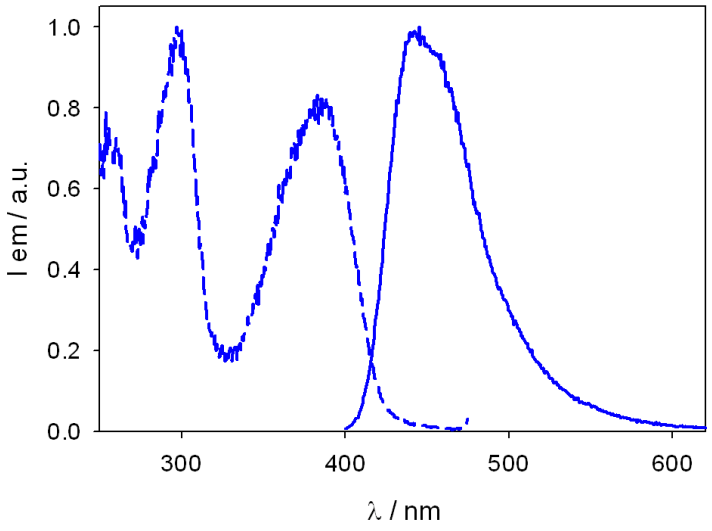

Figure S13. Normalized excitation (dashed line) and emission spectra (solid line) of **NU-1000-BzTz** in H_2O in the presence of excess KCN. λ_{ex}=385 nm; λ_{em}=480 nm.

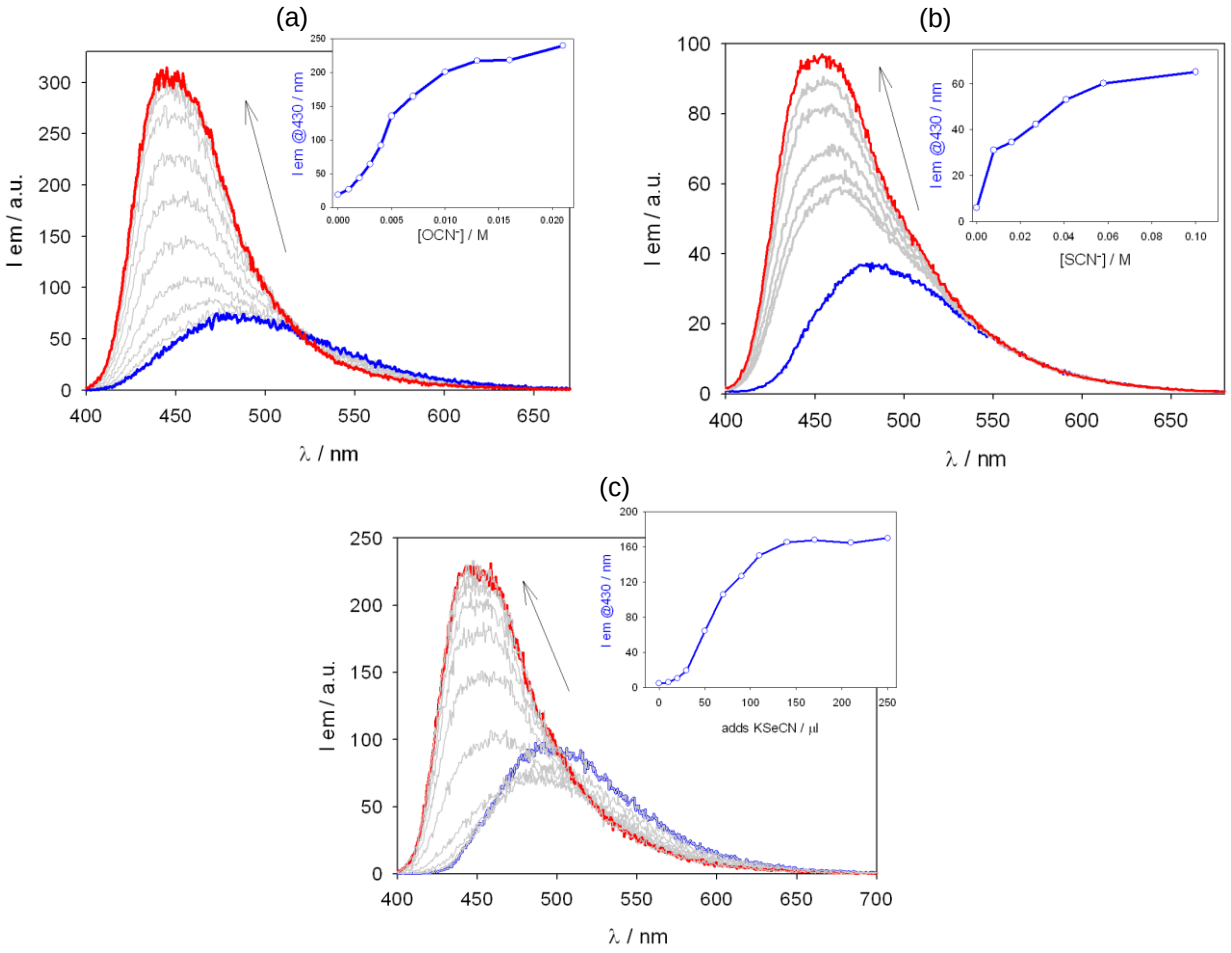

Figure S14. (a) Evolution of the emission spectra recorded for a suspension of **NU-1000-BzTz** upon additions of KOCN (from 0 to *ca.* 21.0 mM, blue to red line, respectively) in H_2O at r.t. λ_{ex}=385 nm; $A_{385nm} \approx 0.24$. Inset: dependence between [OCN^-] and the emission intensity at 430 nm. (b) Evolution of the emission spectra recorded for a suspension of **NU-1000-BzTz** upon additions of NaSCN (from 0 to *ca*. 0.1 M, blue to red line, respectively) in H_2O at r.t. λ_{ex}=385 nm; $0.25 < A_{385nm} < 0.27$. Inset: dependence between [SCN^-] and the emission intensity at 430 nm. (c) Evolution of the emission spectra recorded for a suspension of **NU-1000-BzTz** upon additions of KSeCN (blue to red line, respectively; qualitative) in H_2O at r.t. λ_{ex}=385 nm; $0.24 < A_{385nm} < 0.26$. In the case of KSeCN, a precise calculation of the solution concentration is hampered by the high (and unknown) water content of the hygroscopic salt. Inset: dependence between total additions of $SeCN^-$ and the emission intensity at 430 nm.

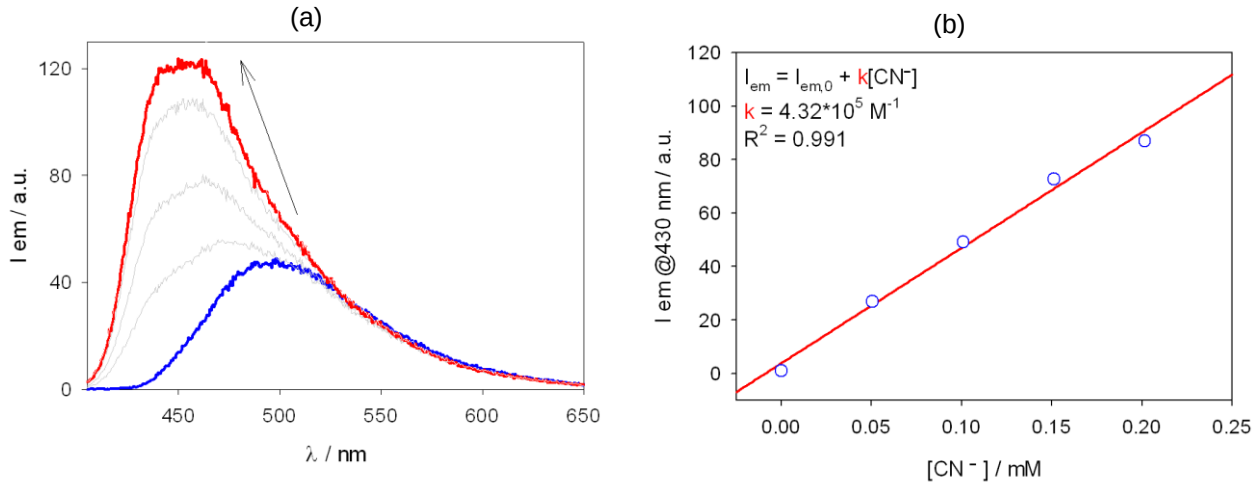

Figure S15. (a) Evolution of the emission spectra recorded for a suspension of **NU-1000-BzTz** upon additions of KCN (from 0 to *ca.* 0.2 mM, blue to red line, respectively) in H_2O at r.t. λ_{ex}=385 nm; 0.32 < A_{385nm} < 0.35. (b) Dependence between [CN^-] and the emission intensity at 430 nm. The slope *k* was calculated with a linear fitting and used to determine the limit of detection (LOD) for the concentration of CN^- (LOD was calculated as LOD=3σ/*k*, where σ is the standard deviation of the intercept and *k* the slope of the linear fitting).[5]

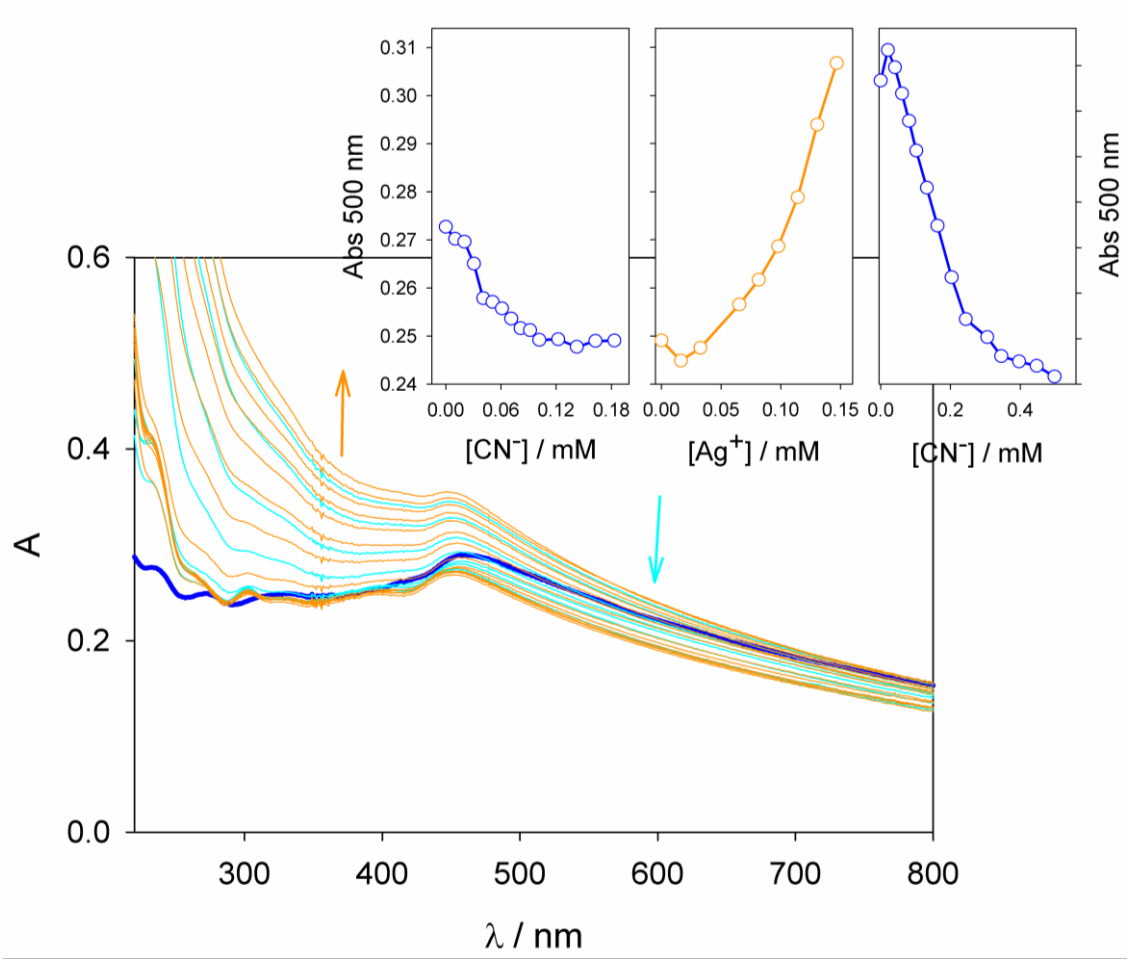

Figure S16. Evolution of the absorption spectra recorded for a suspension of **NU-1000-BzTz** upon additions of KCN (from 0 to *ca.* 0.19 mM, thicker blue to orange line, respectively) in H_2O at r.t. followed by additions of $Ag(CF_3SO_3)$ (up to *ca.* 0.15 mM, thin orange lines). To the so-obtained mixture further amounts of KCN were added (up to total 0.69 mM). Inset: dependence between $[CN^-]$, $[Ag^+]$ and the absorbance at 500 nm.

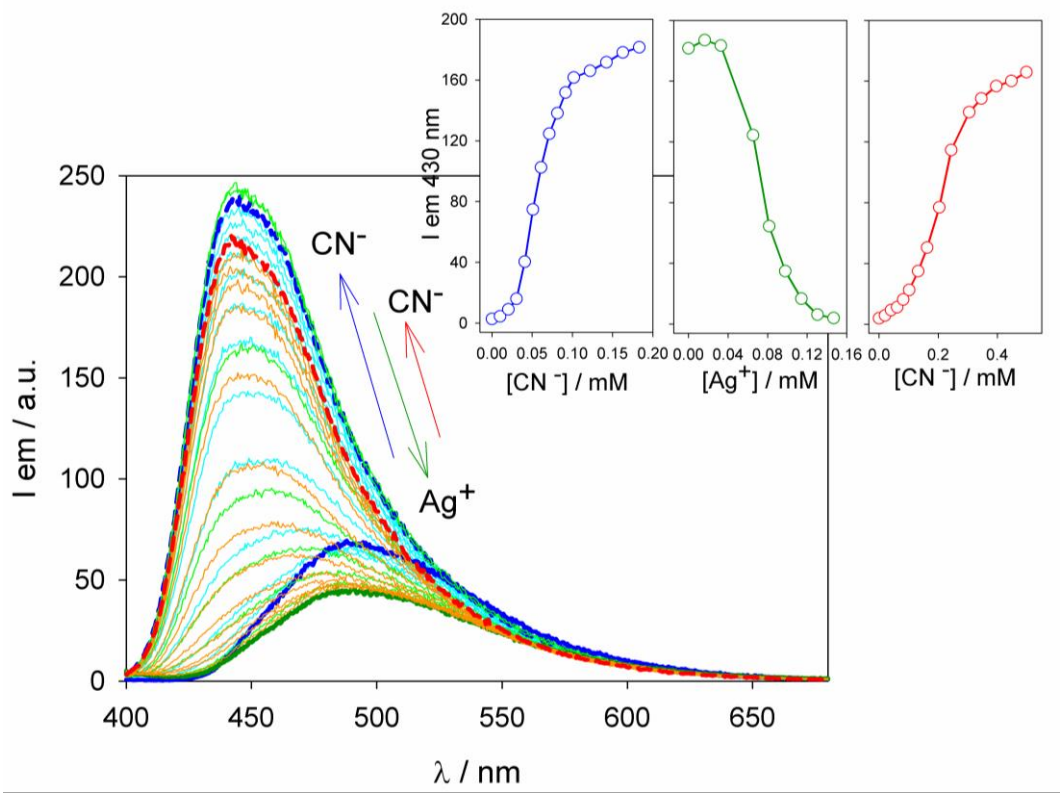

Figure S17. Evolution of the emission spectra recorded for a suspension of **NU-1000-BzTz** upon additions of KCN (from 0 to *ca.* 0.19 mM, blue lines - from solid to dashed, respectively) in H_2O at r.t. followed by additions of $Ag(CF_3SO_3)$ (up to *ca.* 0.15 mM, green lines). To the so-obtained mixture further amounts of KCN were added (up to total 0.69 mM, red lines). Inset: dependence between $[CN^-]$, $[Ag^+]$ and the emission intensity at 430 nm. λ_{ex} = 380 nm.

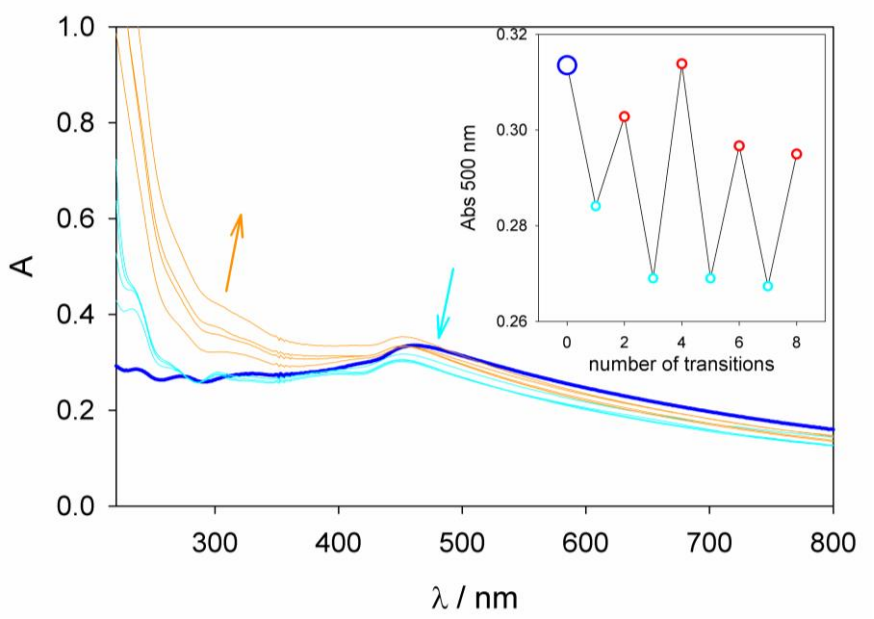

Figure S18. Evolution of the absorption spectra recorded for a suspension of **NU-1000-BzTz** upon repeated additions of KCN (0.4 mM, cyan lines) and Ag(CF_3SO_3) (0.13 mM, orange lines). Inset: absorption at 500 nm upon repeated additions of KCN and Ag(CF_3SO_3).

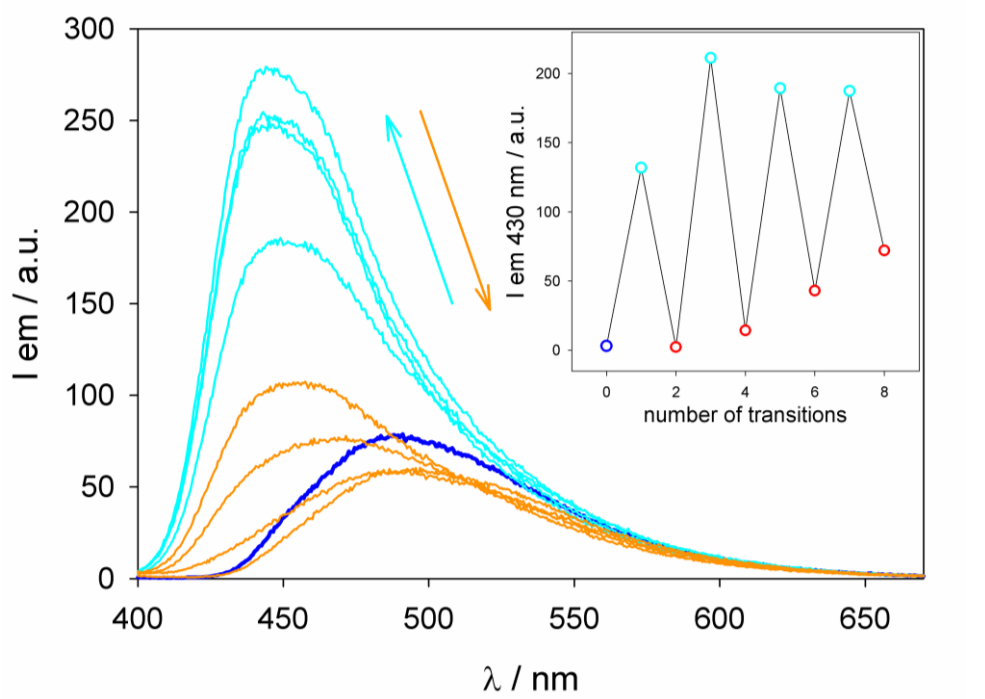

Figure S19. Evolution of the absorption spectra recorded for a suspension of **NU-1000-BzTz** upon repeated additions of KCN (0.4 mM, cyan lines) and Ag(CF_3SO_3) (0.13 mM, orange lines). Inset: fluorescence emission at 430 nm. λ_{ex} = 380 nm.

References

[1] M. C. Burla, R.Caliandro, B. Carrozzini, G. Cascarano, C. Cuocci, C. Giacovazzo, M. Mallamo, A. Mazzone, G. Polidori, *J. Appl. Cryst.* 2015, **48**, 306-309.

[2] G. M. Sheldrick, *Acta Cryst.* 2015, **C71**, 3-8.

[3] M. Nardelli, *Comput. Chem.* 1993**, 7**, 95-98.

[4] L. J. Farrugia, *J. Appl. Cryst.* 1997**, 30**, 565.

[5] A. Karmakar, A. V. Desai, B. Manna, B. Joarder, S. K. Ghosh, *Chem. Eur. J.* 2015, **21**, 7071-7076.